Jurnal Teknologi

Full Paper

SIMULATION OF A SIMPLE VAPOUR-COMPRESSION REFRIGERATION SYSTEM USING R134a

Mohd Yusoff Senawi*, Farah Wahidah Mahmod

Fakulti Kejuruteraan Mekanikal, Universiti Teknologi Malaysia, 81310 UTM Johor Bahru, Johor, Malaysia

Article history
Received
19 May 2016
Received in revised form
7 June 2016
Accepted
30 June 2016

*Corresponding author
myusoff@utm.my

Graphical abstract

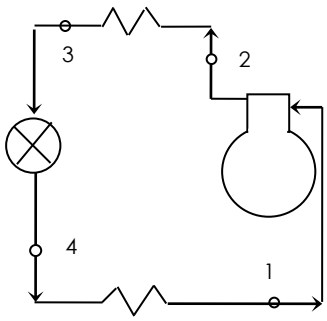

Abstract

A computerized simulation of a simple single-stage vapour-compression refrigeration system has been made. The steady-state simulation uses the accurate property correlations developed by Cleland for refrigerant R134a. The inputs to the program are: evaporator pressure, condenser pressure, superheating at evaporator outlet, subcooling at condenser outlet and compressor isentropic efficiency. The program outputs are: refrigerating effect, compressor work input, coefficient of performance (COP) and suction vapour flow rate per kW of refrigeration. An increase in the evaporator pressure from 150 to 250 kPa improves the COP by 40%. The COP is decreased by 35% when the condenser pressure is increased from 1000 to 1500 kPa. Increasing the superheat at the evaporator outlet from 0 to 16^{0}C improves the COP by 2.6%. An increase in subcooling at the condenser outlet from 0 to 16^{0}C increases the COP by 20%. The COP is improved by 150% when the compressor isentropic efficiency is increased from 0.4 to 1.

Keywords: Refrigeration system, R134a, isentropic efficiency, COP

1.0 INTRODUCTION

The vapour-compression cycle is probably the most widely used basic refrigeration cycle worldwide [1, 2]. R134a is arguably the industry standard refrigerant used in domestic refrigerators and small-size air conditoners. The refigerant has zero ozone depleting potential with a global warming potential (GWP) of 1430. This high GWP is a drawback which will lead to the phasing out of R134a by the year 2030 [3]. As a result, R134a is probably still relevant into the next decade when it will eventually be replaced with a more environmental friendly refrigerant.

Cabello *et al*. [4] have performed an experimental evaluation of the performance of a single-stage vapour compression refrigeration plant which used three different wrorking fluids, R22, R407C and R134a. The operating variables considered were the evaporating pressure, the condensing pressure and the degree of superheating at the compressor inlet. When the compression ratio (ratio of condenser to evaporator pressure) was below 6, the use of R22 resulted in higher coefficient of performance (COP) than when using R407C and R134a. However, at compression ratios greater than 6, the use of both R407C and R134a gave higher COP than when using R22. For all refrigerants, the COP dropped almost linearly with the increase in compression ratio.

Yang and Yeh [5] have performed a numerical study on the performance of vapour-compression systems with R22, R134a, R410A and R717 as refrigerants. The condensing temperature ranged from 40 to 50^{o}C, while the evaporating temperature range was from –20^{o}C to 0^{o}C. It was found that the optimal subcooling was between 2 and 6^{o}C for initial cost saving. On the basis of total exergy destruction, the optimal subcooling was in the range of 4 to 7^{o}C.

Dalkilic and Wongwises [6] have made a theoretical performance study of a vapour-compression refrigeration system using R134a and other refrigerants. The condensing temperature was fixed at 50^{o}C, while the evaporating temperature varied between –30 and 10^{o}C. It was concluded that

the COP increased with an increase in the evaporating temperature.

Computerized simulation of refrigeration cycles require the use of refrigerant thermodynamic property equations. Chan and Haselden [7, 8, 9] have described the development of computer-based refrigerant thermodynamic properties and their application in the computation of standard refrigeration cycles. The technique can be extended to the computerized analysis of many other types of refrigeration cycles as reviewed by Park *et al*. [10].

In this paper, the R134a property correlations developed by Cleland [11] have been used to perform a performance analysis of a theoretical single-stage vapour-compression refrigeration cycle. The theoretical cycle is the simplest approximation to the real cycles [2]. The correlations used are from an extension of the previous work, also by Cleland [12]. The computer program developed in this study enables quantitative analysis to be made accurately on the effects of varying important paramaters on the performance of the cycle.

2.0 METHODOLOGY

The simulation of a simple refrigeration cycle is made using the regression equations of Cleland [11] for refrigerant R134a. The equations enable the calculation of thermodynamic properties such as saturation temperature, and specific enthalpies of saturated liquid, saturated vapour and superheated vapour of R134a. The equations are used to obtain the thermodynamic properties to calculate the refrigerating effect, the compressor work input, the coefficient of performance and the suction vapour flow rate per kW of refrigeration.

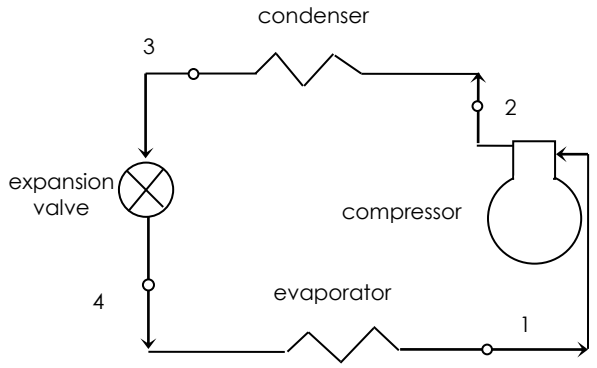

Figure 1 Refrigeration system

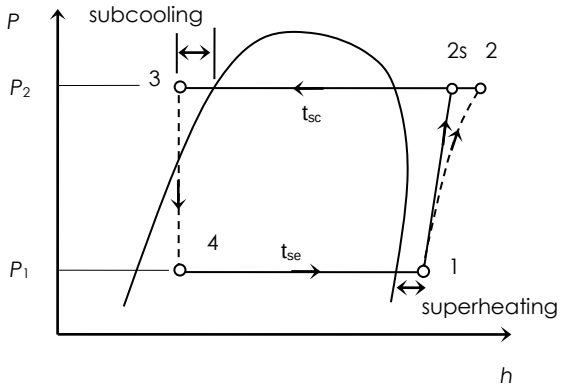

Figure 2 Refrigeration cycle on p-h diagram

Figure 1 shows the schematic diagram of a simple single-stage refrigeration cycle which is made up of a compressor, a condenser, an expansion valve and an evaporator. The corresponding state points are shown in Figure 2 for a typical practical cycle. Superheated vapour enters the compressor at state 1 and is compressed to state 2. From state 2 to state 3, heat is rejected from the high-temperature refrigerant to the surroundings which is at a lower temperature. Compressed liquid refrigerant at state 3 is then throttled isenthalpically to evaporator pressure at state 4. In the evaporator, the low-temperature refrigerant absorbs heat from the surroundings which is at a higher temperature. It is assumed that there are no pressure drops in the evaporator and the condenser.

2.1 Saturation Temperatures

The saturation temperature, t_{se} at the evaporator pressure, p_1 is calculated from Cleland [11],

$$t_{se} = -246.61 - 2200.9809/(\ln(p_1) - 21.51297) \quad (1)$$

while the saturation temperature, t_{sc} at the condenser pressure, p_2 is calculated from [11],

$$t_{sc} = -246.61 - 2200.9809/(\ln(p_2) - 21.51297) \quad (2)$$

2.2 Enthalpy at State 1

When the refrigerant is at the saturated vapour state at the evaporator outlet, the enthalpy at compressor inlet is given by Cleland [11] as follows,

$$h_{i1} = 249455.0 + 606.163*t_{se} - 1.05644*t_{se}^2 - 1.82426e\text{-}2*t_{se}^3$$
$$h_1 = h_{i1} \quad (3)$$

However, for superheated vapour state, the enthalpy is calculated as follows [11],

$$h_1 = h_{i1}*(1 + 3.48186e\text{-}3*dt_1 + 1.6886e\text{-}6*dt_1^2 + 9.2642e\text{-}6*dt_1*t_{se} - 7.698e\text{-}8*dt_1^2*t_{se} +$$

$1.7070e\text{-}7*dt_1*t_{se}^2 - 1.2130e\text{-}9*dt_1^2*t_{se}^2)$ (4)

where,

dt_1 = superheat at state 1 = $t_1 - t_{se}$.

2.3 Enthalpy at State 2s for Saturated Vapour at Compressor Inlet

The enthalpy at state 2 s when the refrigerant is in the saturated vapour state at state 1 is calculated as follows for isentropic compression [11],

$$dt_c = t_{sc} - t_{se} \quad (5)$$

$$ci1 = 1.06469 - 1.6907e\text{-}3*t_{se} - 8.560e\text{-}6*t_{se}^2 - 2.135e\text{-}5*t_{se}*dt_c - 6.1730e\text{-}7*t_{se}^2*dt_c + 2.0740e\text{-}7*t_{se}*dt_c^2 + 7.720e\text{-}9*t_{se}^2*dt_c^2 - 6.103e\text{-}4*dt_c \quad (6)$$

$$c = ci1 \quad (7)$$

$$n = c/(c-1) \quad (8)$$

$$dh = \frac{c}{c-1} * p1 * v_{s1} \left[\left(\frac{p2}{p1} \right)^{\frac{c-1}{c}} - 1 \right] \quad (9)$$

$$h_{2s} = h_1 + dh \quad (10)$$

When c is equal to one, Cleland [11] suggests that c takes a value slightly away from unity (e.g. 1.00001). The saturated vapour specific volume, v_{s1} is given by Cleland [11] as follows,

$$v_{s1} = exp[-12.4539 + 2669.0/(273.15 + t_{se})]* (1.01357 + 1.06736e\text{-}3*t_{se} - 9.2532e\text{-}6*t_{se}^2 - 3.2192e\text{-}7*t_{se}^3) \quad (11)$$

2.4 Enthalpy at State 2s for Superheated Vapour at Compressor Inlet

When there is superheating at state 1, the calculation of h_{2s} follows the method of Cleland [11] for isentropic compression between 1 and 2s.

$$c = ci1*(1.0 + 1.175e\text{-}3*dt_1 - 1.814e\text{-}5*dt_1^2 + 4.121e\text{-}5*dt_1*t_{se} - 8.093e\text{-}7*dt_1^2*t_{se}) \quad (12)$$

$$n = c/(c-1) \quad (13)$$

$$dh = \frac{c}{c-1} * p1 * v_1 \left[\left(\frac{p2}{p1} \right)^{\frac{c-1}{c}} - 1 \right] \quad (14)$$

$$h_{2s} = h_1 + dh \quad (15)$$

where the superheated vapour specific volume, v_1 is given by [11],

$$v_1 = v_{s1}*(1.0 + 4.7881e\text{-}3*dt_1 - 3.965e\text{-}6*dt_1^2 + 2.5817e\text{-}5*dt_1*t_{se} - 1.8506e\text{-}7*dt_1^2*t_{se} + 8.5739e\text{-}7*dt_1*t_{se}^2 - 5.401e\text{-}9*dt_1^2*t_{se}^2) \quad (16)$$

Similarly, c should not equal 1 as mentioned in section 2.3.

2.5 Enthalpy at Compressor Outlet for non-Isentropic Compression

When the compression process is irreversible, the actual enthalpy at compressor outlet is calculated as follows [1],

$$h_2 = h_1 + (h_{2s} - h_1) / \eta_c \quad (17)$$

where η_c is isentropic efficiency of the compressor.

2.6 Liquid Enthalpy

The enthalpy of liquid refrigerant leaving the condenser is calculated from the Cleland [11] equation for the ASHRAE enthalpy datum as follows,

$$h_3 = 50952 + 1335.29*t_3 + 1.70650*t_3^2 + 7.6741e\text{-}3*t_3^3 \quad (18)$$

where, $t_3 = t_{sc} - dt_3$, and for isenthalpic expansion, h_4 is equal to h_3. The subcooling at condenser outlet is denoted as dt_3.

2.7 Performance Calculations

The refrigerating effect, q_{ref} , the compressor work input, w and the coefficient of performance, COP are calculated as follows [1,2,11],

$$q_{ref} = h_1 - h_4 \quad (19)$$

$$w = h_2 - h_1 \quad (20)$$

$$COP = q_{ref} / w \quad (21)$$

The suction vapour flow rate per kW of refrigeration, SVFR is obtained from [6, 13],

$$SVFR = v_1 / q_{ref} \quad (22)$$

The preceding equations have been coded in the C programming language which enables the simulation of a simple single-stage refrigeration cycle to be made. The inputs to the program are: evaporator pressure (p_1), condenser pressure (p_2), degree of superheat at evaporator outlet (dt_1), degree of subcooling at condenser outlet (dt_3) and the isentropic efficiency of the compressor (η_c). The outputs are: refrigerating effect, compressor work requirement, the coefficient of performance and the suction vapour flow rate per kW of refrigeration. The computer program has been validated against the results of Dalkilic and Wongwises [6] where excellent agreements have been obtained.

3.0 RESULTS AND DISCUSSION

In the following case study, the base parameters are set at p_1 = 200 kPa, p_2 = 1300 kPa, dt_1 = 0, dt_3 = 0 and the compressor isentropic efficiency is 100%. In the parametric study, only one parameter is varied while the other parameters remain at the base values.

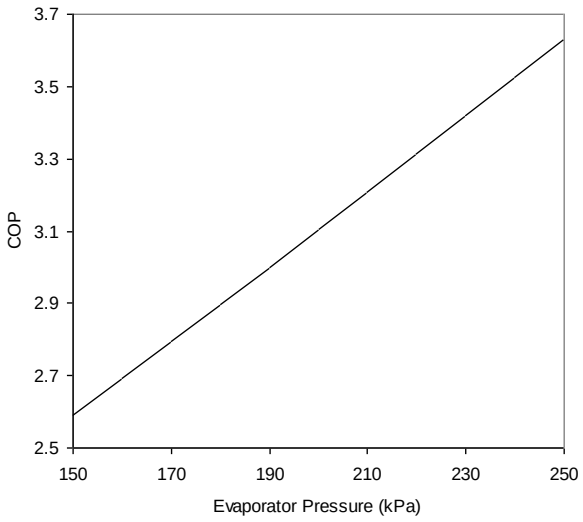

Figure 3 COP versus evaporator pressure

Figure 3 shows that the COP increases by 40% when the evaporator pressure increases from 150 kPa to 250 kPa (evaporating temperature increases from –17.2°C to –4.3°C). As the evaporator pressure increases, the refrigerating effect increases but the compressor work input decreases, resulting in an increase of the COP.

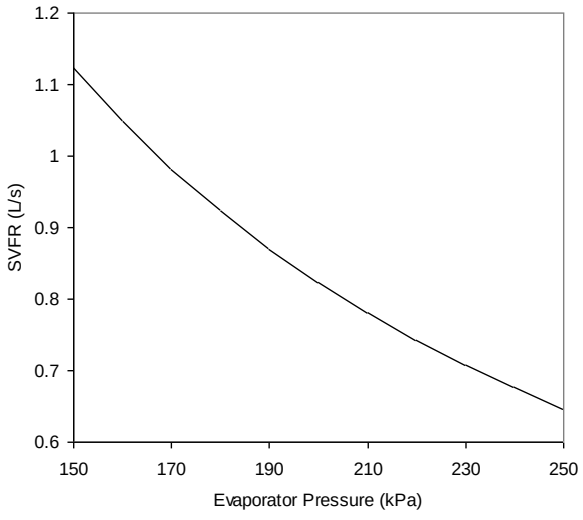

Figure 4 SVFR versus evaporator pressure

Figure 4 shows that the compressor suction volume flow rate (SVFR) decreases by 42% with an increase in the evaporator pressure from 150 kPa to 250 kPa. This is due to the combined effect of increased refrigerating effect and reduced specific volume at compressor inlet when the evaporator pressure increases. An decrease in SVFR simply means a relatively smaller compressor is needed, and as such a low SVFR is most desirable for low capital and operating costs.

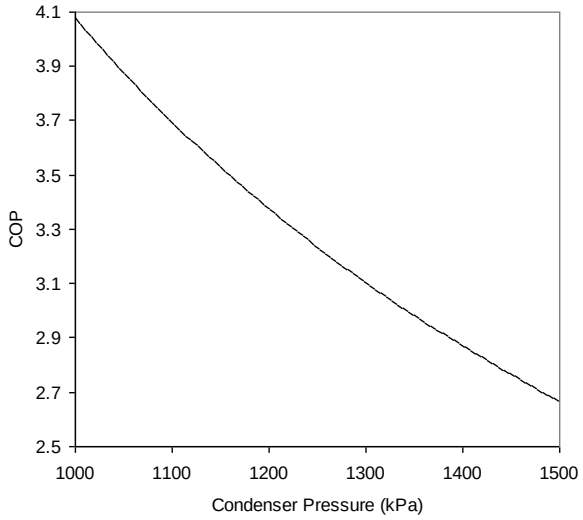

Figure 5 COP versus condenser pressure

Figure 5 shows that the COP decreases by 35% when the condenser pressure increases from 1000 kPa to 1500 kPa (condensing temperature increases from 39.3°C to 55.2°C). This is due to the combined effect of decreased refrigerating effect and increased compressor work input when condenser pressure increases.

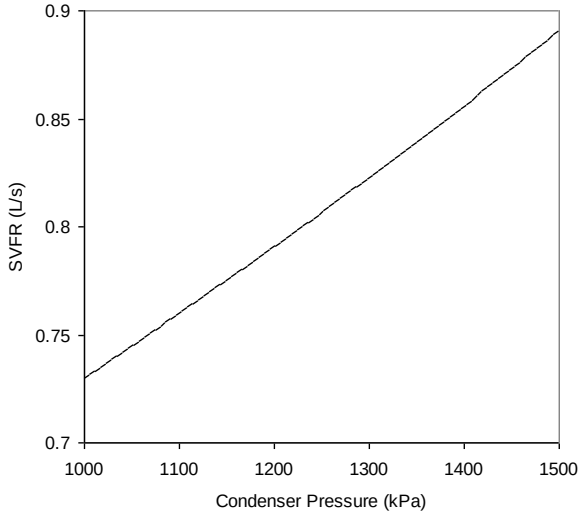

Figure 6 SVFR versus condenser pressure

When the condenser pressure increases from 1000 to 1500 kPa, the SVFR increases by 22% as shown in Figure 6. In this case, the refrigerating effect

decreases with increased condenser pressure, while the specific volume at compressor inlet remains at a constant value, resulting in the almost linear increase in SVFR with an increase in condenser pressure.

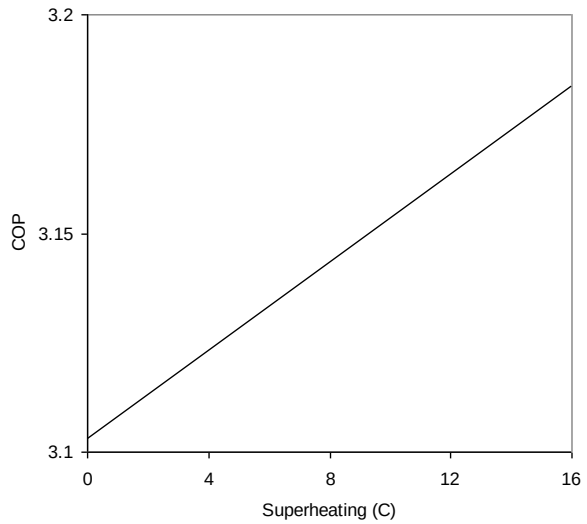

Figure 7 COP versus superheating

Figure 7 shows that there is a marginal increase in the COP by about 2.6% as the superheat at compressor inlet is increased from 0 to 16°C. Even though the refrigerating effect and the compressor work input increase with superheating, the increase in refrigerating effect is slightly more dominant, resulting in a slight increase in COP with superheating at compressor inlet.

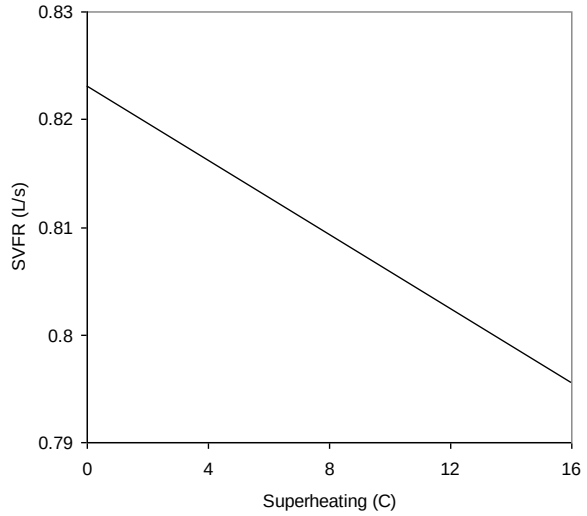

Figure 8 SVFR versus superheating

By increasing the amount of superheat from 0 to 16°C, the SVFR decreases linearly from 0.823 to 0.796 L/s (3.3% decrement) as shown in Figure 8. Although both refrigerating effect and specific volume at compressor inlet increase with the amount of superheat, the increase in refrigerating effect is more dominant, resulting in a slight reduction in SVFR.

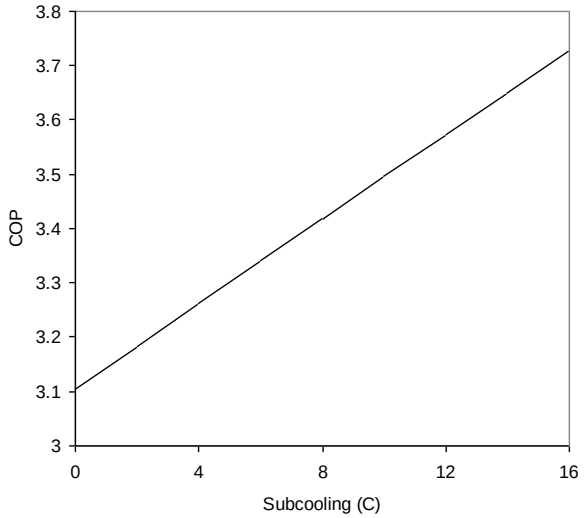

Figure 9 COP versus subcooling

Figure 9 shows that the COP increases by 20% when subcooling at the condenser outlet is increased from 0 to 16°C. In this case, the compressor work input is not affected by the amount of subcooling, but the refrigerating effect is increased with an increase in subcooling, resulting in a significant increase in the COP.

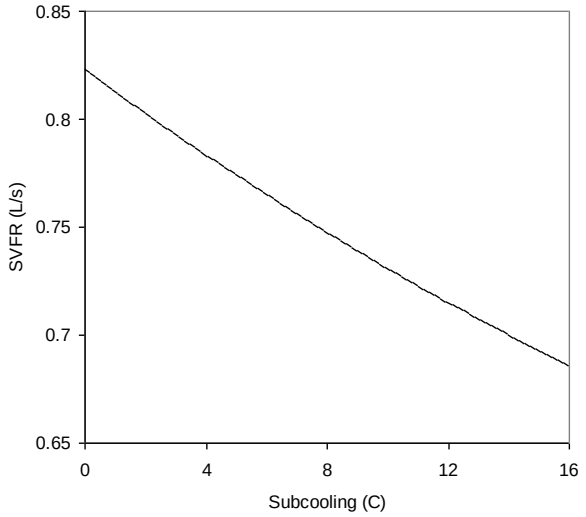

Figure 10 SVFR versus subcooling

The SVFR decreases with an increase in subcooling as shown in Figure 10. It decreases by 17% as subcooling is increased from 0 to 16°C. Subcooling has no effect on the specific volume at compressor inlet, but the refrigerating effect increases with subcooling which results in reduced SVFR when the amount of subcooling is increased.

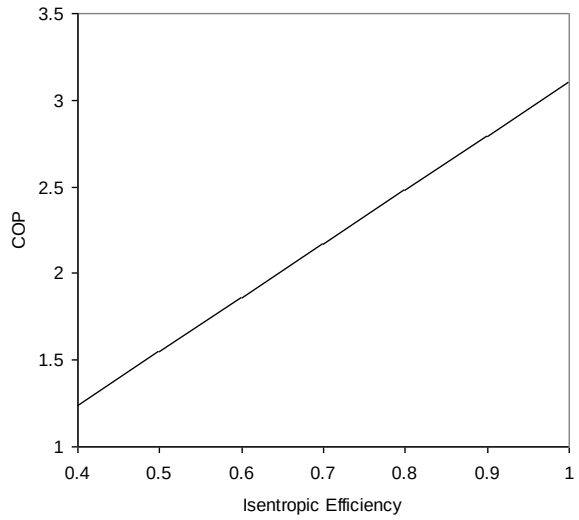

Figure 11 COP versus compressor isentropic efficiency

Figure 11 shows that the COP increases linearly with the isentropic efficiency of the compressor. The COP increases by 150% when the efficiency increases from 0.4 to 1. The refrigerating effect is not affected by the efficiency, but the compressor work input is significantly reduced when the compressor becomes more efficient, which explains the observed trend.

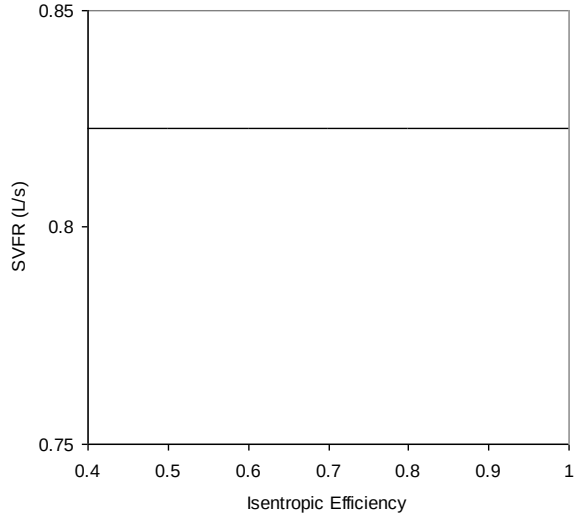

Figure 12 SVFR versus compressor isentropic efficiency

The isentropic efficiency of the compressor has no effect on both the refrigerating effect and the specific volume at the compressor inlet which results in a constant SVFR of 0.823 L/s as shown in Figure 12.

4.0 CONCLUSION

The property correlations for R134a developed by Cleland [11] have been used to develop a simulation program for a simple vapour-compression refrigeration cycle. A case study has been made for a typical cycle and the effects of some parameters on the performance of the cycle have been studied. The COP increases with an increase in the evaporator pressure, but decreases with an increase in the condenser pressure. An increase in the amount of superheating results in a marginal increase of COP. However, increased subcooling results in a substantial increase of the COP. An increase in compressor isentropic efficiency results in a significant increase of the COP. An increase in the evaporator pressure results in a reduction of the SVFR. However, increased condenser pressure causes the SVFR to increase. An increase in superheating at the compressor inlet reduces the SVFR marginally. However, an increase in subcooling at the condenser outlet reduces the SFVR quite substantially. The compressor isentropic efficiency has no effect on SVFR. The findings in this study are consistent with the qualitative analysis by Arora [13].

Nomenclature

ASHRAE	American Society of Heating, Refrigerating and Air Conditioning Engineers
COP	coefficient of performance
dt_1	superheat at compressor inlet, ^{0}C
dt_3	subcooling at condenser outlet, ^{0}C
h	specific enthalpy, J/kg
p	absolute pressure, Pa
q_{ref}	refrigerating effect, J/kg
SVFR	suction vapour flow rate per kW refrigeration, m^3/s
t	temperature, ^{0}C
t_{se}	evaporating temperature, ^{0}C
t_{sc}	condensing temperature, ^{0}C
v	specific volume, m^3/kg
w	compressor work, J/kg

Greek symbols

η_C	compressor isentropic efficiency

Subscripts

c	condenser
e	evaporator
s	saturation
2s	outlet of isentropic compressor
1	compressor inlet
2	compressor outlet
3	condenser outlet
4	evaporator inlet

Acknowledgement

This research was supported by Universiti Teknologi Malaysia.

References

[1] Stoecker, W. F., and J. W. Jones. 1982. *Refrigeration and Air Conditioning*. 2nd Edition. New York: McGraw-Hill Book Company.

[2] McQuiston, F. C., J. D. Parker, and J. D. Spitler. 2005. *Heating, Ventilating, and Air Conditioning: Analysis and Design.* 6th Edition. New York: John Wiley & Sons, Inc.

[3] Kabeel, A. E., A. Khalil, M. M. Bassuoni, and M. S. Raslan. 2016. Comparative experimental study of low GWP alternative for R134a in a walk-in Cold Room. *International Journal of Refrigeration*. 69: 303-312.

[4] Cabello, R., E. Torrello, and J. Navarro-Esbri. 2004. Experimental Evaluation Of A Vapour Compression Plant Performance Using R134a, R407C and R22 As Working Fluids. *Applied Thermal Engineering*. 24: 1905-1917.

[5] Yang, M. H., and R. H. Yeh. 2015. Performance And Exergy Destruction Analyses Of Optimal Subcooling For Vapor-Compression Refrigeration Systems. *International Journal of Heat and Mass Transfer*. 87: 1-10.

[6] Dalkilic, A. S., and S. Wongwises. 2010. A Performance Comparison Of Vapour-Compression Refrigeration System Using Various Alternative Refrigerants. *International Communications in Heat and Mass Transfer*. 37: 1340-1349.

[7] Chan, C. Y., and G. G. Haselden. 1981. Computer-based Refrigerant Thermodynamic Properties. Part 1: Basic Equations. *International Journal of Refrigeration*. 4: 8-12.

[8] Chan, C. Y., and G. G. Haselden. 1981. Computer-based Refrigerant Thermodynamic Properties. Part 2: Program Listing. *International Journal of Refrigeration*. 4: 52-60.

[9] Chan, C. Y., and G. G. Haselden. 1981. Computer-based Refrigerant Thermodynamic Properties. Part 3: Use Of The Program In The Computation Of Standard Refrigeration Cycles. *International Journal of Refrigeration*. 4: 131-134.

[10] Park, C., H. Lee, Y. Hwang, and R. Radermacher. 2015. Recent Advances In Vapor Compression Cycle Technologies. *International Journal of Refrigeration*. 60: 118-134.

[11] Cleland, A. C. 1994. Polynomial Curve-Fits For Refrigerant Thermodynamic Properties: Extension To Include R134a. *International Journal of Refrigeration*. 17(4): 245-249.

[12] Cleland, A. C. 1986. Computer Subroutines For Rapid Evaluation Of Refrigerant Thermodynamic Properties. *International Journal of Refrigeration*. 9: 347-351.

[13] Arora, C. P. 2000. *Refrigeration and Air Conditioning*. 2nd Edition. New Delhi: Tata McGraw-Hill Publishing Company Limited.